ISSN: 2277-9655
Impact Factor: 4.116

IJESRT

INTERNATIONAL JOURNAL OF ENGINEERING SCIENCES & RESEARCH TECHNOLOGY

ELLIPTICAL REFLECTIVE CAVITY TO COUPLE A BURNER WITH A RECEIVER

P. Sansoni[1*], D. Fontani[1], F. Francini[1], D. Jafrancesco[1], G. Toniato[2]
[1]CNR-INO National Institute of Optics, Largo E. Fermi, 6 – Firenze - 50125 - Italy-
Phone. +39-055-23081; Fax. +39-055-2337755
[2]Business Consultant for Riello Group, via Ing. Pilade Riello 7, 37045, Legnago, Italy
Phone +39-3357271866

DOI: 10.5281/zenodo.160850

ABSTRACT

A reflective elliptical cavity is analysed to couple a cylindrical burner with a receiver made of three arrays of thermophotovoltaic cells. The advantage of the elliptical shape is that burner and receiver can be placed in the two foci of the ellipse; while in the circular cavity they should be both placed in the centre. The elliptical cavity is studied as component for a thermo-electric cogenerator of thermophotovoltaic type, considering practical requirements and realisation constraints. Ray-tracing analyses examine received power, collection efficiency and irradiance distribution; in particular the uniformity of the light focused on the receiver is very important to maximise the thermophotovoltaic conversion. The research compares the elliptical reflective cavity with the circular cavity, for various distances between burner and receiver. Increasing diameters of the burner are considered in the elliptical cavity, choosing the best solution. An ideal-diffusion reflector is considered to realise the cavity walls, instead of a specular-reflection material.

KEYWORDS: optical design, thermophotovoltaic, reflector, cogeneration.

INTRODUCTION

This work concerns the development of a thermo-electric micro-cogeneration system of ThermoPhotoVoltaic (TPV) type. It is a Combined Heat and Power system (CHP system) to be realized by integrating a condensing boiler for residential use with appropriate photovoltaic (PV) cells [1-2].

In general thermophotovoltaic systems for this type of applications use PV cells placed in close proximity to a heat source, that typically operates between 700 and 1600 ° C, for the conversion of thermal energy into electrical energy [3-7]. Thanks to the high ratio between the capturing surface and the total volume, such systems allow to obtain a ratio of power per unit volume more favourable compared to other technological solutions. Since the radiation to be converted is in the infrared (IR) region, the photovoltaic cells used in these specific applications are all based on semiconductors with low *band-gap* (or *energy gap*, Eg) [2,5], whose absorption wavelengths are around 1-5 μm.

In order to maximize the conversion efficiency is necessary, not only select appropriately the individual components of the thermophotovoltaic micro-cogenerator (emitter, photoconverter, plus any filters, mirrors and concentrators of the electromagnetic radiation), but also carefully design the overall system and identify the optimal working conditions [8]. For instance, Qiu et al. have developed a TPV system with cells in gallium antimonide (GaSb) and comparative tests indicate that the performance of the PV cells and, in particular, the produced power density, changes significantly varying the combustor / emitter configuration and the combustion parameters [9]. The comparative study of Fraas et al. describes the significant performance variations achieved for three different TPV systems employing cells in Si, GaSb and InGaAs / InP [2]. Note that the use of different types of cell necessarily requires to reconsider also the characteristics of the other components of the system. The two cases outlined above clearly demonstrate that the identification of a suitable photoconverter for a specific TPV application cannot be made *a-priori*, solely based on the technical characteristics of the cells. In fact the various components of a system of thermo-electric cogeneration influence each other, to an extent dependent on the operating conditions used.

A classical configuration for a TPV generator is the cylindrical layout: the cells are connected together in linear arrays arranged radially around the emitter [10]. Employing silicon cells and an itterbia emitter the produced energy costs 0.19 Euro / kWh, with efficiencies of about 2% and power density of around 0.2 W / cm^2; moreover performance improvements are possible using filters, concentrators of radiation or heat recovery systems [8,11-14]. The maximum temperatures of use on the basis of current technical knowledge and legislation, are generally limited to 1500 ° C [11]. However detailed analysis of the energy flows of this TPV generator evidence that only a small part of emitted radiation is absorbed by the PV cells generating useful electric power. As alternative to the traditional cylindrical configuration, this paper proposes an elliptical shape for the reflective cavity containing emitter and absorber. In this elliptical cavity the burner (almost a cylinder) is placed in the first focus of the ellipse and the array of PV cells is near the second focus.

If the combustor / emitter presents an emission spectrum of black / grey body type, a substantial fraction of the photons absorbed by the PV cell would not produce electricity, but simply an unwanted overheating of the cell. In this situation is generally necessary to interpose between the emitter and the cell an appropriate filter capable of shielding the fraction of photons ineffective for the thermoelectric conversion [15,16]. By the way, if you are using a porous burner, the filter also has the function of preventing the convective transfer of heat and of avoiding the combustion products from contaminating the cell surface [5,9]. Conversely, if the emitter / combustor emits selectively at an energy next to the band-gap of the PV cell used, the thermal load on the cell is significantly reduced and no filter is needed. A selective emission can, for example, be obtained by using ceramic materials based on oxides of the rare earths such as Yb2O3, Er2O3, Ho2O3 or Nd2O3 that, thanks to their peculiar electronic structure, emit very specific wavelengths in the IR range [2,8,12,17,18]. In order to avoid damage and minimise losses in efficiency, the cells are usually cooled to temperatures below 50-60 ° C [2,12].

Crucial to the efficiency of thermoelectric conversion is, in particular, the matching between the wavelength of the emission maximum of the emitter and the band-gap of the PV cell. Such a result may be achieved, at least in principle, by acting on the characteristics of the combustor / emitter (first selecting suitable materials that constitute it and controlling the working temperature), the cell (using semiconductor with suitable Eg value), and any other components (filters, mirrors, concentrators, ...) in order to optimize the so-called "spectral control" [2,6,17,13,19].

In the scientific literature thermophotovoltaic systems are conventionally classified into three categories, namely low (T < 1100 ° C), medium (1100 ° C < T <1400 ° C) and high (T > 1400 ° C) temperature, in dependence of the working conditions of the emitter and therefore depending on its spectral characteristics. In conclusion, each of these temperature ranges presupposes the use of photovoltaic cells with appropriate band-gap.

Besides, any commercial success of a specific TPV application depends not only on the electrical performance that it is able to ensure and on the overcoming of technical difficulties, but also on the cost of the technology itself. From this point of view, silicon is certainly the most economical material and readily available. In the case of cells in GaSb, Fraas et al. have estimated that the cost of this semiconductor may decrease with increasing production volumes following a trend parallel to that of the silicon market [1,2]. On the basis of this trend, if you consider the cost of produced energy (in $ / watt), in equal volumes of production the gallium antimonide is about a hundred times cheaper than silicon. Much more uncertain is the analysis of costs for other III-V ternary or quaternary semiconductors. As such materials are produced with epitaxial techniques it is realistic to assume that their cost remains significantly higher than that of GaSb. The commercial success of these materials is also further hindered by the fact that their production requires the use of toxic gases [2,6].

SIMULATION OF THE ELLIPTICAL CAVITY

The reflective cavity with elliptical section is proposed as alternative to the simple cylindrical assembly used to construct a thermo-electric cogenerator [20-22]. Since the two foci of the ellipse are coupled, they allocate burner and TPV receiver, so the reflective walls of the cavity concentrate the radiation emitted by the burner in the other focus of the ellipse where a suitable receiver converts thermal energy into electricity. The elliptical reflective cavity was simulated staring from the technical constraints dictated by the foreseen practical construction of the TPV micro-cogenerator. The cavity is a metallic cylinder with elliptical base, the burner has tubular shape and the TPV receiver has tubular shape with triangular section. Figure 1 presents the scheme of the reflective cavity, seen from the top, indicating the main elements and reporting the dimensions (in mm).

The components fundamental for the collection of radiation are only 3: burner, reflective cavity and photoconverter. Figure 2 shows a 3D-rendering drawing only these components. The burner is a hollow cylinder with diameter 2 cm, height 20 cm, and emission surface 125.7 cm^2; it has an uniform emission over the entire outer lateral surface, with

Lambertian distribution, with grey body spectrum with emissivity 0.7, blackbody temperature of 1470 K, emission band 0.8 - 1.8 μm, emitted power density (calculated on emission band) 3.6 W / cm^2, total power emitted 452.2 W. The cavity is a tube of elliptical section, with two holes on the upper and lower plates in correspondence of the emitter, with major axis of 27.5 cm, minor axis 25.2 cm, focal length (distance transmitter - receiver) 11 cm, height 21.7 cm, upper hole diameter 4 cm, lower hole diameter 5 cm; its surface reflectance characteristics are as "Alanod MIRO High Reflectance 95" (reflectance between 0.95 and 0.99 in the emission band). The receiver is composed of 3 arrays of TPV cells, with width 2 cm (horizontal side), height 20 cm (vertical side), and a completely absorbing surface of 40 cm^2. To take into account also the effects of the supports that are necessary for practical reasons, the simulations include emitter base, receiver base and support of the cells arrays, all considered fully absorbent. The emitter base is a hollow cylinder, perforated on the upper surface, with diameter 5 cm, hole diameter 4 cm, height 0.8 cm. The receiver base is a hollow cylinder of diameter 5.7 cm and height 0.8 cm. The triangular receiver support is a tube with triangular section of side 2.1 cm and height 20.9 cm.

These ray-tracing analyses (using the *Zemax-EE* package by *Radiant Zemax*) are addressed to optimise the geometrical configuration of the elliptical cavity. The starting ellipse is selected with some preliminary estimations and considering the requirements of the optical manufacturing of the reflective walls. The purpose of the simulations is to analyse the performance of radiation collection of the cavity, so the quantities examined are total power focused on the cells arrays and their irradiance profiles. The triangular receiver contains 3 linear detectors: D1, D2 and D3, as shown in Fig. 1. The results of the radiation focused on each detector is considered along the horizontal side and along the vertical side. The dimensions indicated in Fig. 1 are all in mm; the interdistance *d* between burner and receiver is 110 mm.

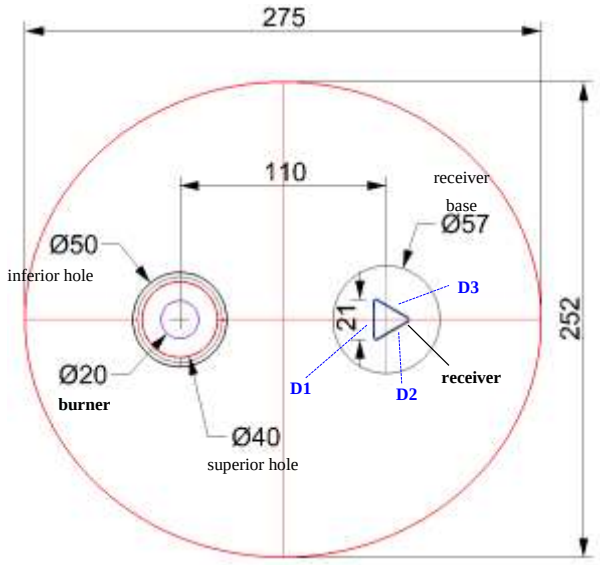

Fig. 1 - Top view of the elliptical cavity with detectors D1, D2 and D3 "pointing right".

ISSN: 2277-9655
Impact Factor: 4.116

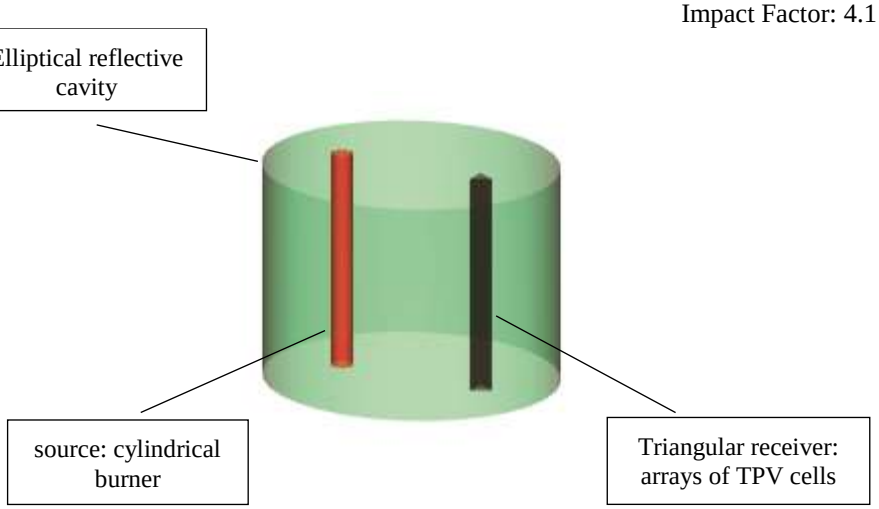

Fig. 2 - 3D-rendering of the reflective elliptical cavity with receiver "pointing right".

Some initial simulations compared the configurations with triangular receiver as in Fig. 1 ("pointing right") or rotated of 180° ("pointing left"). The total collection efficiency was 62% for receiver "pointing right" and 61% "pointing left". The focused radiation was more uniformly distributed on the detectors (especially for D2 and D3) "pointing left"; in this case D1 faced the right wall of the ellipse, while D2 and D3 faced the burner but inclined. The configuration "pointing right" had D1 in front of the burner and the others facing the opposite part, and the irradiance fluctuated along the horizontal side of D2 (or D3). These fluctuations did not allow TPV cells to reach their optimal performance. Another ray-tracing study considered a variation of the reflectance *R* of the elliptical cavity walls: *R* was set to a 0.9 (for every wavelength and incidence angle), while in the original simulation it was between 0.95 and 0.99 ("Alanod MIRO High Reflectance *R* 95" of *Zemax*). The results were lower collection efficiency (55%) for *R*=0.9, but similar irradiance profiles along both detector sides. Other preliminary simulations examined the consequences of inserting quartz protections around burner and/or receiver. The effect was only on the collection efficiency, which was reduced from 62% to 55% with burner protection, to 54% with receiver protection, and to 48% inserting both protections. The irradiance profiles on the detectors, studied on horizontal and vertical directions, did not change when the protections were added. From these initial simulations it can be concluded that cavity walls reflectance and protections on emitter or receiver affect the collection efficiency, and consequently the focused power. Accurate optical finishing should maximise the walls reflectance; while for the cells surface, maybe suitable coating could reduce the losses. Regarding the performance of the cells, a crucial aspect is the irradiance profile along the cells arrays that the initial studies showed to be quite uniform along the vertical side (with a little loss due to receiver and burner bases), while the profile on horizontal side is less homogeneous.
These preliminary simulations were taken as starting point and reference for more detailed ray-tracing studies. The optical evaluations were still based on the power level focused on the TPV receiver, on the collection efficiency and on the irradiance profiles of the radiation reflected on the 3 linear detectors. The research work proceeded with simulations analysing the performance of the TPV cavity by making the following changes to the original model (in Figures 1-2):

- replacement of the elliptical cavity with a circular one of diameter 265 mm;
- variation of the diameter of the emitter cylinder;
- replacement of the specular-reflection material with ideal-diffusion reflector.

CIRCULAR CAVITY WITH FIXED COMPONENTS

In the first modified configuration the elliptical reflective cavity is replaced with a circular one (Fig. 3), retaining the remaining features of the simulation. So the material of cavity walls, the positions of emitter and receiver and all other parameters of the model remain unchanged with respect to the elliptical cavity studied in the initial studies (Figures 1-2). As in the initial simulations of the elliptical cylinder, also this circular cylindrical cavity has two holes on the lower and upper surfaces in correspondence of the burner. The model used in the simulations is displayed in Figures 3-4. Figure 3 shows a top view of the reflective cavity with circular base. In case of elliptical section, burner and receiver were placed in the ellipse's foci, while this is impossible when the section is a circle. Figure 4 shows a

3D-rendering of the circular cavity containing burner, burner base, triangular receiver and receiver base. The receiver is still composed of three linear arrays of TPV cells and it is placed as in Fig. 1 ("pointing right" layout). The dimensions indicated in Fig. 3 are all in mm. The interdistance *d* between burner and receiver is set to 110 mm, as in the elliptical cavity of Fig. 1.

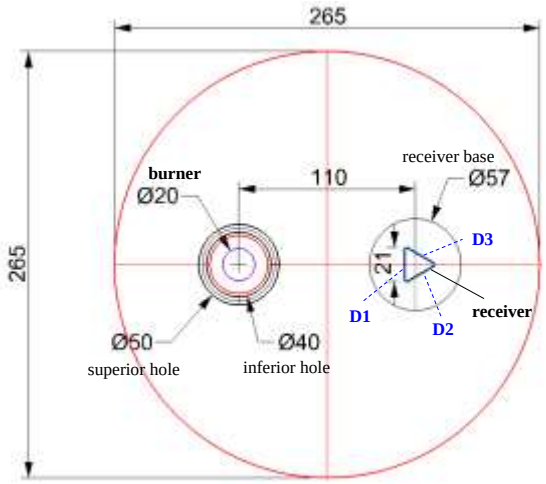

Fig. 3 - Top view of the circular cavity with receiver "pointing right".

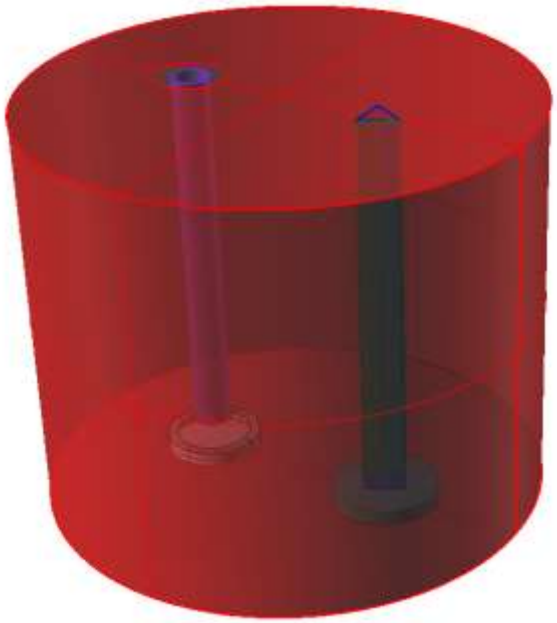

Fig. 4 - 3D rendering of the complete model, with circular shape and receiver "pointing right".

The parameters of the circular cavity are:
• cylindrical cavity of circular base, with two holes on the upper and lower plates to match with the burner
• diameter of 26.5 cm
• burner - receiver distance 11 cm
• height of 21.7 cm
• diameter of superior hole 4 cm

• diameter of inferior hole 5 cm
• surface reflectance characteristics as Alanod MIRO High Reflectance 95 (reflectance between 0.95 and 0.99 in the emission band)

In the simulations the power and irradiance are computed on the three rectangular detectors, forming the triangular receiver, considering the entire area covered with arrays of cells, thus including any spaces between the cells, which in the real case are ineffective surfaces. The detectors were named D1, D2 and D3, and are shown in the figures to allow the distinction. The profiles were evaluated on the horizontal side (of length 2 cm) or along the vertical side (of length 20 cm) of each detector.
Table 1 shows results for circular cavity with fixed interdistance d = 110 mm between burner and receiver. In order to make a comparison between circular cavity and elliptical cavity, the table presents the corresponding data pertaining to the elliptical shape. The columns report the power emitted P_{em}, the power P_{D1}, P_{D2} and P_{D3} collected by the three detectors, the total power collected P_{TOT} and the total efficiency of collection η, defined as $\eta = P_{TOT}/P_{em}$.

Table 1: Collected power and collection efficiency.

Cavity Shape	P_{em} *(W)*	P_{D1} *(W)*	P_{D2} *(W)*	P_{D3} *(W)*	P_{TOT} *(W)*	□ *(%)*
Circular cavity with *d*=110mm	452.4	56.0	38.0	38.1	132.1	29.2
Elliptical cavity with *d*=110mm	452.4	120.4	80.8	80.8	281.9	62.3

The collection efficiency when the cavity section is a circle is less than half the value obtained with elliptical section for the cylindrical reflective cavity (of Fig. 1). As previously observed, the elliptical cavity permits to place the burner in the first focus and the receiver in the second focus of the ellipse. But when these two foci coincide, in the circular cylindrical cavity, the two internal components still need to have a minimum distance for practical reasons. The optimisation of this interdistance between burner and receiver is the next step of this research.

CIRCULAR CAVITY WITH MOVABLE COMPONENTS

The reason of the low efficiency value in the circular cavity with fixed components is due to the distance between emitter and receiver. In fact, given that a circle is an ellipse with zero eccentricity, the two foci coincide with its centre. It is expected the maximum collection efficiency when the burner and receiver are placed both in the centre, which is not physically possible. Hence dedicated simulations evaluated the collection efficiency for different interdistances between the two components.
To make a meaningful comparison the cavity with fixed components, described in the previous section, is replaced with an identical one but without holes, since otherwise it would be necessary to design each time a cavity with holes in correspondence of the burner. The variation parameter is the interdistance *d*: as Fig. 5 illustrates, the distance *d* is considered from the centre of the circular burner to the barycentre of the triangular receiver. Simultaneously to these two components, the respective bases are repositioned, thus the bases are maintained in the same relative position with respect to burner and receiver.

ISSN: 2277-9655
Impact Factor: 4.116

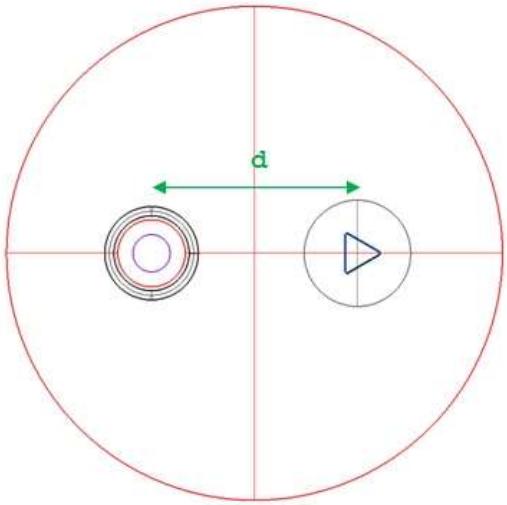

Fig. 5: The interdistance d is the parameter varied in these simulations.

Figures 6-7 and Table 2 present the results calculated for various interdistances *d*: the power collected by detector D1, D2 and D3 (indicated in Fig. 3), the total collected power and the total efficiency of collection η. The figures give an overview of how the examined quantities vary when the burner-receiver distance increases. The table numerically reports the most significant data: the results for d = 110 mm refers to the distance studied in Sect. 3 (results shown in Table 1), while d = 60 mm represents the best situation (at least from a point of view of the radiation collection).

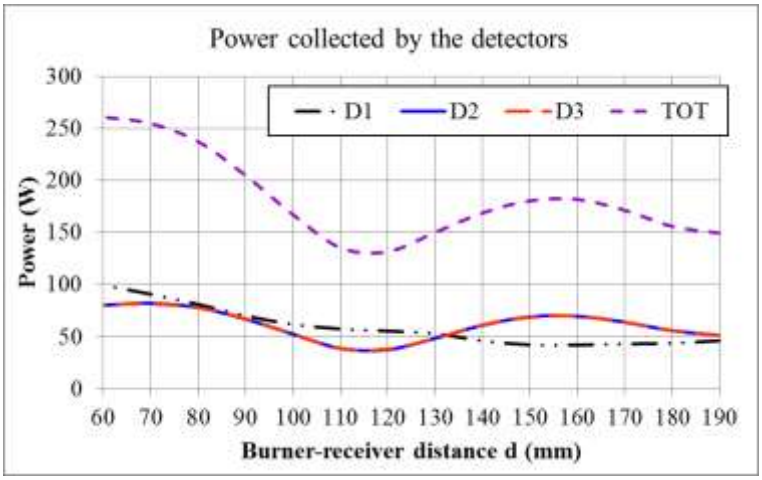

Fig.6: Circular cavity - Power collected by the detectors as a function of d.

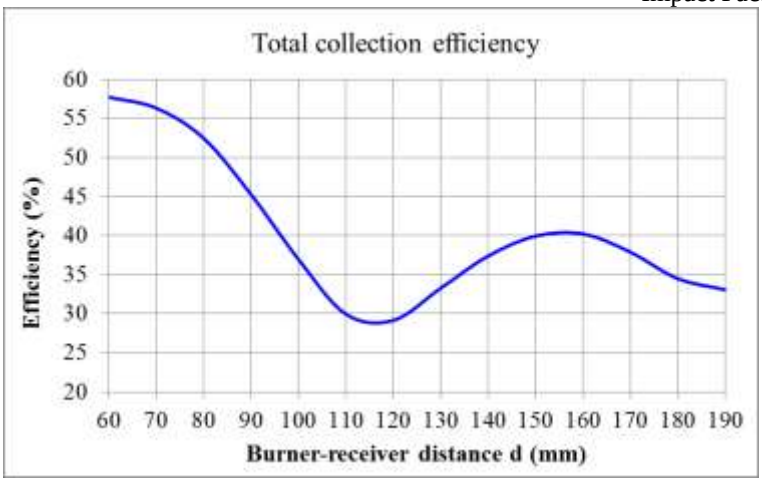

Fig. 7: Circular cavity – Total collection efficiency as a function of d.

Table 2: Circular cavity - Collected power and collection efficiency.

d *(mm)*	P_{D1} *(W)*	P_{D2} *(W)*	P_{D3} *(W)*	P_{TOT} *(W)*	η *%*
110	57.7	38.9	39.0	135.5	30.0
60	99.6	80.5	80.8	260.9	57.7

Considering the case with d = 110 mm, the efficiency did not change significantly, despite the use of a closed cavity, going from 29% of Table 1 (with holes, visible in Fig. 3) to 30% of Table 2 (without holes).
Figure 6 illustrates the performance of the collected power (total and for the three detectors individually) as a function of the distance d between burner and receiver. The absolute maximum for the collected power corresponds to the limit d → 0, i.e. at the centre of the cavity. This is in perfect agreement with the observation made at the end of Sect. 3: in the circle the two foci of the ellipse coincide with the centre. In the elliptical cavity (in Sect. 2) there was only one maximum for the total collected power, which corresponded to the burner and receiver positioned in the two foci on the ellipse (in Fig. 1). In the circular cavity with movable components there is a second maximum, although lower, at $d \approx 160$ mm, where the collection of the rear detectors D2 and D3 slightly increases.
To complete the results for the circular cavity, Fig. 7 plots how the total collection efficiency, defined as the ratio between the total power collected and the emitted power, varies as the interdistance d increases. Even in the position of maximum collection, in which the bases of the burner and receiver are almost in contact, the collection efficiency and total power are slightly lower than those obtained with the configuration of the elliptical cavity (in Fig.1): efficiency 62% and power 282W. The maximum values obtained in the circular cavity, for d = 60 mm, are efficiency 58% and total power 261 W.
It is interesting to compare all the results of the circular cavity with d = 60 mm, representing the best case, with the data of the elliptical cavity where d = 110 mm, the exact distance between the two foci. To have a meaningful comparison in all simulations burner characteristics, features and orientation of the triangular receiver are the same of the initial configuration, named in Sect. 2 elliptical cavity with detectors “pointing right” (Fig. 1).
Considering the irradiance distribution on the three detectors, Figures 8-9 report the profiles as a function of the distance from the centre of the detector. Figure 8 plots the irradiance profiles along the horizontal side, while Fig. 9 reports the distribution in the vertical direction of each detector. In both configurations, for symmetry, detectors D2 and D3 have the same irradiance profile, vertically and horizontally along the receiving surface. For the vertical distribution, all profiles are almost flat with a slow decrease at the left extreme, in correspondence of the bases of the components. The horizontal profiles show very different behaviours among the two cavities and the detectors. As expected, the irradiance profile along D1 is almost symmetrical with respect to the axis of the detector, and its value is almost constant in the elliptical cavity, while it fluctuates in the circular cavity. So the array of cells D1 could be illuminated uniformly in the elliptical cavity, while it would be illuminated more unevenly in the circular one. Unfortunately the situation of uneven illumination of linear detectors D2 and D3 occurs in both cavities. The

horizontal profile of D2 (or D3) is completely asymmetrical and, more important, the irradiance varies from 1 to 2.5 with elliptical or circular shape.

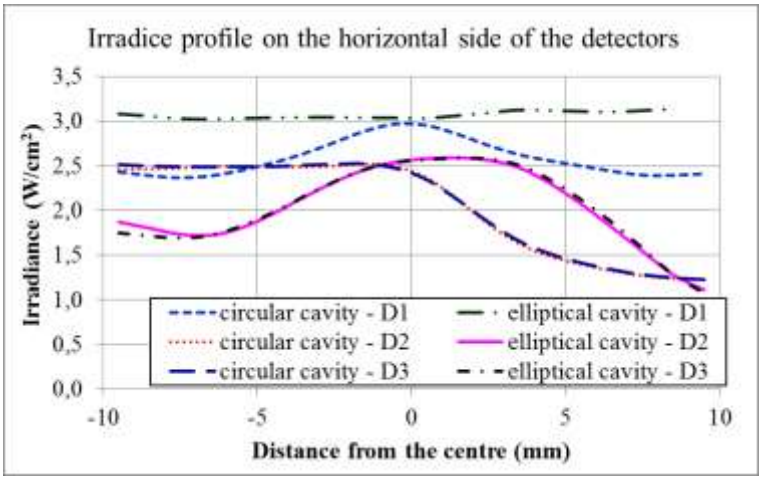

Fig. 8 - Horizontal distribution for circular cavity (with d=60mm) and elliptical cavity (with d=110mm).

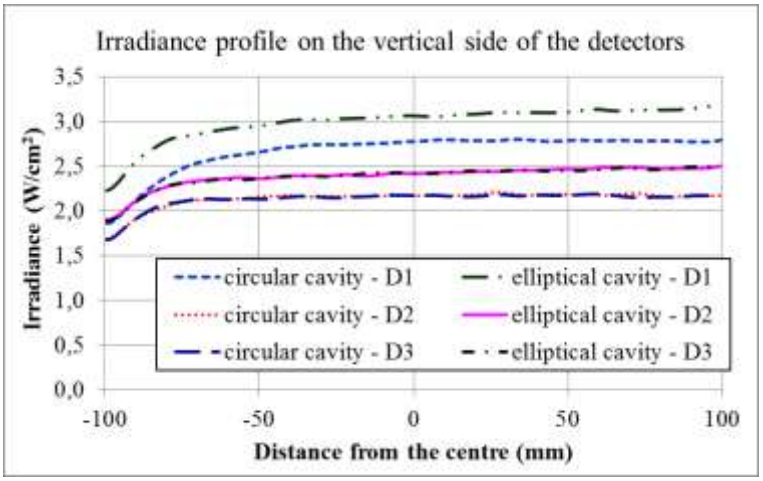

Fig. 9 - Vertical distribution for circular cavity (with d=60mm) and elliptical cavity (with d=110mm).

CHANGE OF BURNER SIZE IN THE ELLIPTICAL CAVITY

The research proceeded with a study dedicated to the effects obtained varying the diameter of the cylindrical burner in the original elliptical cavity of Fig. 1. The stating point is the configuration considered in the initial simulations discussed in Sect. 2: the elliptical cavity with detectors “pointing right”. The variation parameter in this case is the diameter of the emitting cylinder; all other parameters remain unchanged.

For each value of the diameter considered the total power emitted is recalculated maintaining constant the power density value of 3.6 W / cm^2, determined by considering an emission of grey body with the parameters indicated in Sect. 2.

Figures 10-11 and Table 3 shows the simulation results. The original configuration of Fig. 1 in Sect. 2 has a burner diameter of 20 mm, this is the starting value, which corresponds to a total collection efficiency of 62%, considering the triangular receiver “pointing right”. When the burner is enlarged, the emitted power rises because the emitting surface is enlarged. As a consequence the power collected by each detector increases, as well as the total received power, but the total collection efficiency decreases. Therefore for the collection efficiency, the best condition in the elliptical cavity is with burner diameter 20 mm, the configuration of Fig. 1.

ISSN: 2277-9655
Impact Factor: 4.116

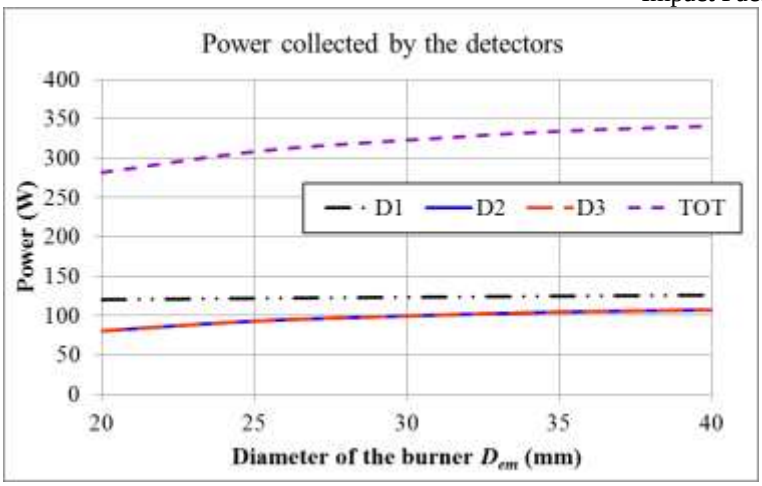

Fig. 10: Elliptical cavity – Behaviour of received power as a function of burner size D_{em}.

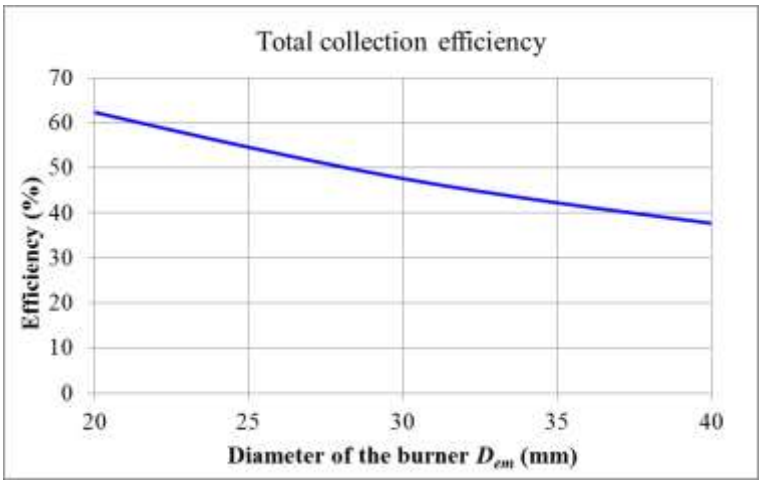

Fig. 11: Elliptical cavity – Behaviour of total collection efficiency as a function of D_{em}.

Figures 10-11 illustrate the behaviour of collected power and total collection efficiency as a function of the diameter of the burner in the elliptical cavity. Figure 10 indicates that the collected power increases with the enlargement of D_{em}, since it enhances the emitted power. On the contrary, the trend of the collection efficiency is opposite. Figure 11 shows that the total efficiency decreases when the burner is enlarged, because widening the emitter increases the fraction of light that does not impinge on the receiver.
Table 3 compares the data obtained for the two extreme diameters: the columns report, from left to right, the burner diameter (D_{em}), the emitter surface (S_{em}), the emitted power (P_{em}), the power collected by the three detectors (P_{D1}, P_{D2}, P_{D3}), the total power (P_{TOT}) and the total collection efficiency η.

Table 3: Elliptical cavity - Collected power and collection efficiency.

D_{em} (mm)	S_{em} (cm^2)	P_{em} (W)	P_{D1} (W)	P_{D2} (W)	P_{D3} (W)	P_{TOT} (W)	η %
20	125.7	452.4	120.5	80.7	80.7	282.0	62.3
40	251.3	904.8	126.3	107.4	107.5	341.2	37.7

The behaviour of collected power is a slightly increasing curve, while the trend of collection efficiency is a rapidly decreasing curve, whose values go from 62 to 37 doubling the burner diameter. Hence doubling the size of the burner augments the total collected power of 21% but reduces the total collection efficiency of 40%.

The results are completed by the irradiance profiles as a function of burner size: the most interesting plots are the profiles along the horizontal side of each detector. The vertical profiles are very similar to those displayed in Fig. 9, so they are not shown. For burner diameter of 20, 30 and 40 mm, Figures 12-14 present the profiles of irradiance on the short side of the receivers (of width 2 cm).

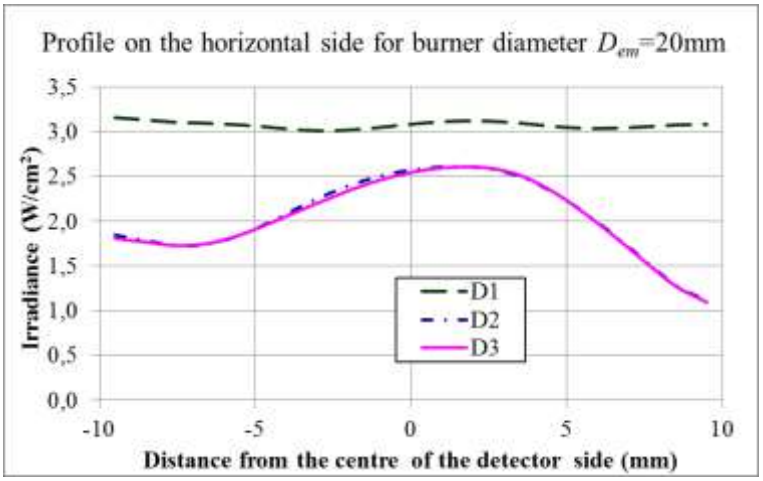

Fig. 12: Elliptical cavity – Irradiance profile on the horizontal side for D_{em} = 20 mm.

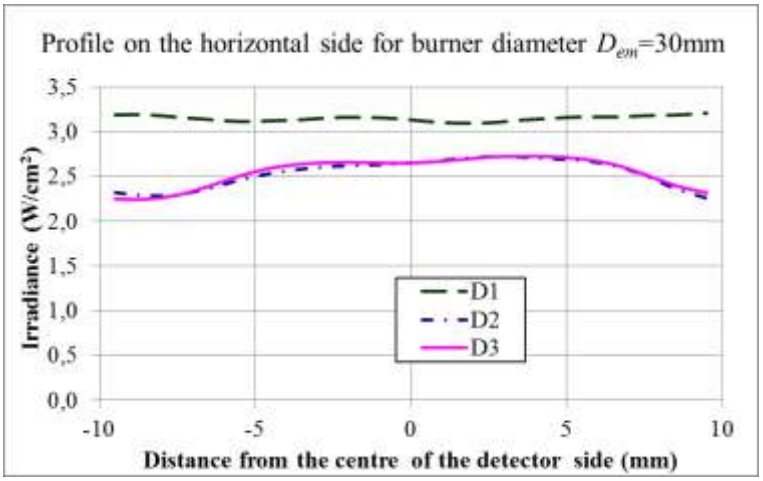

Fig. 13: Elliptical cavity – Irradiance profile on the horizontal side for D_{em} = 30 mm

ISSN: 2277-9655
Impact Factor: 4.116

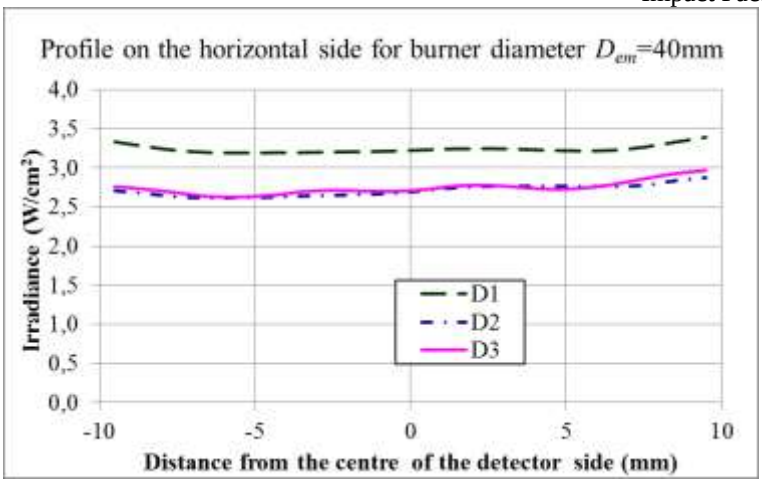

Fig. 14: Elliptical cavity – Irradiance profile on the horizontal side for D_{em} = 40 mm.

Even if the efficiency is reduced, the enlargement of the emitter size has positive effects on the uniformity of illumination of the detectors in the horizontal direction. The irradiance profiles show less fluctuations as the burner diameter grows, and for D_{em} = 40 mm they become almost flat.

DIFFUSIVE ELLIPTICAL CAVITY

The material of the cavity walls can be an ideal-diffusion reflector instead of a specular-reflection material. This possibility is investigated with a dedicated simulation where the reflective material ("Alanod MIRO High Reflectance *R* 95") is replaced with a perfect diffusive reflector. The geometry is identical to the reflective elliptical cavity described in Section 2 and sketched in Figures 1-2: all the optical parameters, except the walls reflectance *R*, remain unchanged. The cavity walls are simulated in *Zemax* as a "perfect diffusive reflector": this is an ideal material, with reflectance $R = 0.9999$ (total) independent from the wavelength, with *Lambertian* diffusion profile.
The results obtained for the diffusive elliptical cavity are compared in Table 4 to the corresponding results of the reflective cavity. The columns report the power emitted P_{em}, the power P_{D1}, P_{D2} and P_{D3} collected by the three detectors, the total power collected P_{TOT} and the total efficiency of collection η.

Table 4: Collected power and collection efficiency.

Cavity type	P_{em} *(W)*	P_{D1} *(W)*	P_{D2} *(W)*	P_{D3} *(W)*	P_{TOT} *(W)*	□ *(%)*
Diffusive elliptical cavity	452.4	61.4	50.4	50.3	162.1	35.8
Reflective elliptical cavity	452.4	120.4	80.8	80.8	281.9	62.3

The use of a diffusive material reduces drastically the power collected on the triangular receiver, because in the diffusive case the light is not conveyed on it but is spread uniformly in all directions. Compared to the case with specular reflective material, the efficiency is almost halved, falling from 62% to 36%.
Since the triangular receiver is made of arrays of thermophotovoltaic cells, the illumination of these linear arrays (D1, D2 and D3), in both directions, is very important. An uneven distribution of the radiation on the receiver surface can cause low conversion levels and may also damage the cells themselves. Figures 15-16 plot the irradiance profiles on two sides of the detectors: for the short horizontal side in Fig. 15, for the long vertical side in Fig. 16. The uniformity is high for the diffusive power of the material, but the values are very low: are around 1.5 W / cm^2. On the other hand, the elliptical cavity with walls in "Alanod MIRO High Reflectance *R* 95" focuses 3 W / cm^2 on the detector D1, and values between 1.5 and 2.5 W / cm^2 for D2 and D3. However, as previously noted, the elevated uniformity of the radiation focused on the receivers is a great advantage using TPV cells.

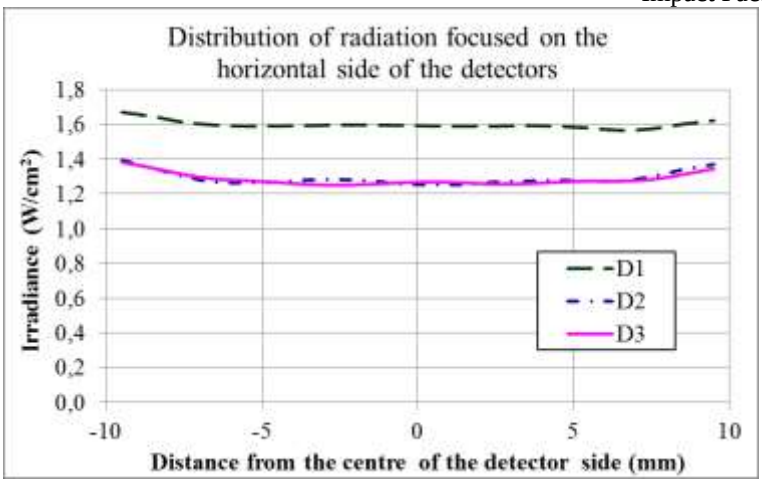

Fig. 15: Elliptical cavity – Irradiance profile on the horizontal side.

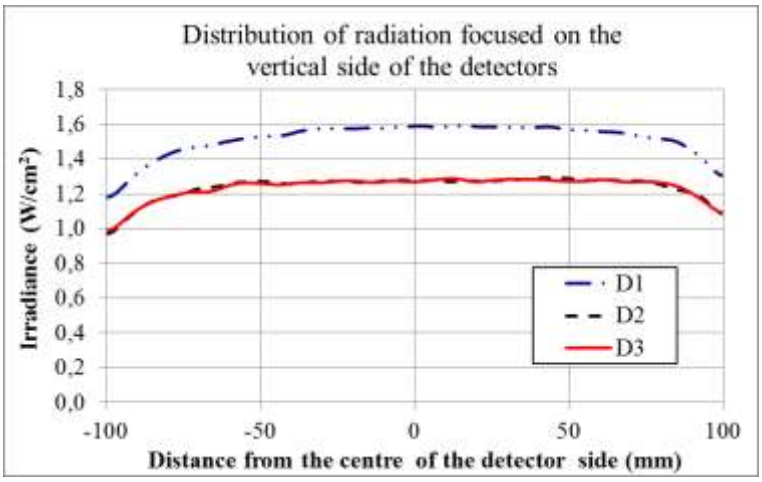

Fig. 16: Elliptical cavity – Irradiance profile on the vertical side.

CONCLUSION

A reflective cylindrical cavity with elliptical section is studied to couple a burner with a photoconverter. The shape of the burner is a cylinder; while the receiver is composed of 3 arrays of ThermoPhotoVoltaic cells (TPV cells). The advantage of using an elliptical cavity that burner and receiver can be placed in the two foci of the ellipse. Some initial simulations have defined suitable geometrical parameters for the elliptical cavity in order to maximize the received power and to take into account the constraints of construction. Also the orientation of the receiver, which is a tube with triangular section, has been optimised. The three linear components of the triangular receiver, the TPV cells arrays, are indicated as “detectors”.

Starting from this reference configuration, ray-tracing analyses consider various modifications of the elliptical reflective cavity: circular shape, change of burner-receiver distance, various sizes of the burner, diffusive walls of the cavity. The research examines collected power (in total or on every detector) and collection efficiency, but also the irradiance profile on the 3 detectors, which should be as uniform as possible to maximise the conversion performed by the TPV cells [23].

This concentrating chamber is studied as component for a combined heat and power micro-cogenerator that should combine proper TPV cells with a condensing boiler for residential use [22, 24-27]. The construction restrictions and practical requirements are taken into account in the simulation in order to have a model as realistic as possible [20-21]. The reference configuration for the elliptical cavity was developed with the final purpose of realising a prototype. Figure 17 illustrate the practical realization of this thermo-electric cogenerator of thermophotovoltaic type.

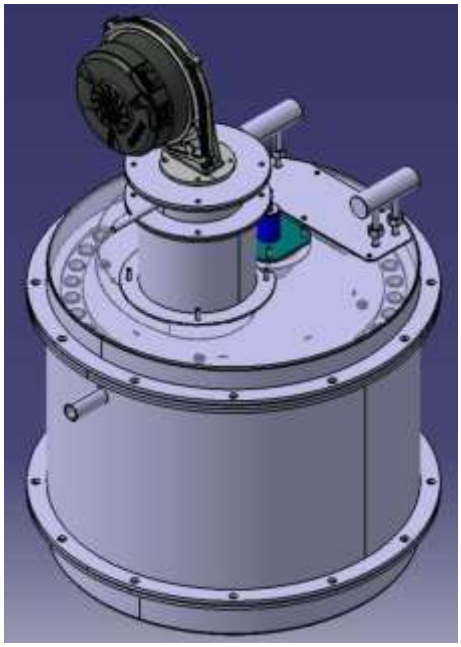

Fig. 17: Thermo-electric micro-cogeneration system of ThermoPhotoVoltaic (TPV) type.

The modification of the cavity geometry from the elliptical cylinder to a circular cylinder leads to a decrease of collection efficiency. In the circular cavity the two ellipse's foci are coincident and therefore the physical distance between burner and receiver does not allow an efficient transfer of radiation between the two components. The irradiance profiles indicate that the problem of uneven illumination (especially in the horizontal direction, short side) of the detectors is not solved by changing the cavity shape from ellipse to circle.

In the circular cavity, a successive study varies the interdistance *d* between burner and receiver, starting from the value (*d*=110mm) of the reference elliptical cavity. Receiver power and collection efficiency increase as the distance *d* decreases, in agreement with the coincidence of the two foci of the ellipse that become the centre of the circle. For practical reasons burner and receiver need to have a minimum interdistance (*d*=60mm), which corresponds to maximum efficiency and maximum received power in the circular cavity.

In the elliptical cavity, the total collected power does not increase linearly with the diameter of the cylindrical burner, since the enlargement of the diameter reduces the collection efficiency (more light is generated but it is also wasted more). On the contrary, a reduction in the burner diameter would improve the efficiency of collection, at the cost of a decrease in collected power and partial illumination of the receiver. The advantage of enlarging the burner size is to have more uniform irradiance profiles along the horizontal detector side.

The use of a diffusive reflecting material for the elliptical cavity walls, even ideal, is not suitable for the application to cogeneration systems, in which the aim is to illuminate a very small surface area (the arrays of TPV cells) in comparison to the overall size of the cavity. One such material, spreading the light, distributes it in a wide area, thus improving the uniformity of illumination on the TPV cells, but decreasing the collection efficiency.

Regarding the simulation of the arrays of TPV cells, more accurate results could be obtained taking into account in the simulation the actual spaces between the cells, that do not contribute to the collection of radiation useful for the photovoltaic conversion.

ACKNOWLEDGMENTS

The study has been developed in the framework of the project "PIACE – Intelligent, integrated and adaptive platform of micro-cogeneration with high efficiency for residential use", a research project financed by the *Italian Ministry of Economic Development* within the programme "Industry 2015 – Energetic Efficiency" with prime proposer RIELLO SpA.

REFERENCES

[1] L. M. Fraas, J. E. Avery, H. X. Huang, "Thermophotovoltaic furnace–generator for the home using low bandgap GaSb cells," Semicond. Sci. Technol., vol. 18, pp. S247-S253, 2003.
[2] L. M. Fraas, J. E. Avery, H. X. Huang, R. U. Martinelli, "Thermophotovoltaic system configurations and spectral control," Semicond. Sci. Technol., vol. 18, pp. S165-S173, 2003.
[3] R. W. Miles, K. M. Hynes, I. Forbes, "Photovoltaic solar cells: An overview of state-of-the-art cell development and environmental issues," Progr. Cryst. Growth Charact. Mater., vol. 51, pp. 1-42, 2005.
[4] N. N. Lal, A. W. Blakers, "Sliver cells in thermophotovoltaic systems," Sol. Energy Mater. Sol. Cells, vol. 93, pp. 167-175, 2009.
[5] G. Colangelo, A. de Risi, D. Laforgia, "New approaches to the design of the combustion system for thermophotovoltaic applications," Semicond. Sci. Technol., vol. 18, pp. S262-S269, 2003.
[6] R. G. Mahorter, B. Wernsman, R. M. Thomas, R. R. Siergiej, "Thermophotovoltaic system testing," Semicond. Sci. Technol., vol. 18, pp. S232-S238, 2003.
[7] R. S. Tuley, R. J. Nicholas, "Band gap dependent thermophotovoltaic device performance using the InGaAs and InGaAsP material system," J. Appl. Phys., vol. 108, pp. 084516/1-084516/7, 2010.
[8] B. Bitnar, Silicon, "Germanium and silicon/germanium photocells for thermophotovoltaics applications," Semicond. Sci. Technol., vol. 18, pp. S221-S227, 2003.
[9] K. Qiu, A. C. S. Hayden, "Thermophotovoltaic generation of electricity in a gas fired heater: Influence of radiant burner configurations and combustion processes," Energy Convers. Manage., vol. 44, pp. 2779-2789, 2003.
[10] T. J. Coutts, "A review of progress in thermophotovoltaic generation of electricity," Renewable Sustainable Energy Rev., vol. 3, pp. 77-184, 1999.
[11] G. Palfinger, B. Bitnar, W. Durisch, J.-C. Mayor, D. Grützmacher, J. Gobrecht, "Cost estimate of electricity produced by TPV," Semicond. Sci. Technol., vol. 18, pp. S254-S261, 2003.
[12] K. Qiu, A. C. S. Hayden, "Development of a silicon concentrator solar cell based TPV power system," Energy Convers. Manage., vol. 47, pp. 365-376, 2006.
[13] T. J. Coutts, G. Guazzoni, J. Luther, "An overview of the fifth conference on thermophotovoltaic generation of electricity," Semicond. Sci. Technol., vol. 18, pp. S144-S150, 2003.
[14] B. Bitnar, W. Durisch, J.-C. Mayor, H. Sigg, H.R. Tschudi, "Characterization of rare earth selective emitters for thermophotovoltaic applications," Sol. Energy Mater. Sol. Cells, vol. 73, pp. 221-234, 2002.
[15] K. Qiu, A. C. S. Hayden, M.G. Mauk, O.V. Sulim, "Generation of electricity using InGaAsSb and GaSbTPV cells in combustion-driven radiant sources," Sol. Energy Mater. Sol. Cells, vol. 90, pp. 68-81, 2006.
[16] O. Vigil, C. M. Ruiz, D. Seuret, V. Bermúdez, E. Diéguez, "Transparent conducting oxides as selective filters in thermophotovoltaic devices," J. Phys. Condens. Matter, vol. 17, pp. 6377-6384, 2005.
[17] M. Ghanashyam Krishna, M. Rajendran, D. R. Pyke, A. K. Bhattacharya, "Spectral emissivity of Ytterbium oxide-based materials for application as selective emitters in thermophotovoltaic devices," Sol. Energy Mater. Sol. Cells, vol. 59, pp. 337-348, 1999.
[18] Timothy J. Coutts, "An overview of thermophotovoltaic generation of electricity," Sol. Energy Mater. Sol. Cells, vol. 66, pp. 443-452, 2001.
[19] F. O'Sullivan, I. Celanovic, N. Jovanovic, J. Kassakian, S. Akiyama, K. Wada, "Optical characteristics of one-dimensional Si/SiO2Si/SiO2 photonic crystals for thermophotovoltaic applications," J. Appl. Phys., vol. 97, pp. 033529/1-033529/7, 2005.
[20] M. Schubnell, P. Benz, J.C. Mayor, "Design of a thermophotovoltaic residential heating system," Sol. Energy Mater. Sol. Cells, vol. 52, pp. 1-9, 1998.
[21] Keith W. Lindler, Mark J. Harper, "Combustor/emitter design tool for a thermophotovoltaic energy converter," Energy Convers. Manage., vol. 39, pp. 391-398, 1998.
[22] S. K. Chou, W. M. Yang, K. J. Chua, J. Li, K. L. Zhang, "Development of micro power generators–a review," Appl. Energy, vol. 88, pp. 1-16, 2011.
[23] K. Qiu, A. C. S. Hayden, "Performance of low bandgap thermophotovoltaic cells in a small cogeneration system," Solar Energy, vol. 74, pp. 489-495, 2003.

[24] Yueh-Heng Li, Hong-Yuan Li, Derek Dunn-Rankin and Yei-Chin Chao, "Enhancing Thermal, Electrical Efficiencies of a miniature combustion-driven thermophotovoltaic system," Prog. Photovolt: Res. Appl., vol. 17, pp. 502-512, 2009.
[25] Yueh-Heng Li, Yung-Sheng Lien, Yei-Chin Chao and Derek Dunn-Rankin, "Performance of a Mesoscale Liquid Fuel-film Combustion-driven TPV Power System," Prog. Photovolt: Res. Appl., vol. 17, pp. 327-336, 2009.
[26] H. J. Sheen, W. J. Chen, S. Y. Jeng, T. L. Huang, "Correlation of swirl number for a radial-type swirl generator," Experimental Thermal and Fluid Science, vol. 12, pp. 444-451, 1996.
[27] S. Martemianov, V.L. Okulov, "On heat transfer enhancement in swirl pipe flows," International Journal of Heat and Mass Transfer, vol. 47, pp. 2379-2393, 2004.